

On the subgroup structure of the hyperoctahedral group in six dimensions

Emilio Zappa,^{a,c*} Eric C. Dykeman^{a,b,c} and Reidun Twarock^{a,b,c}^aDepartment of Mathematics, University of York, York, UK, ^bDepartment of Biology, University of York, York, UK, and ^cYork Centre for Complex Systems Analysis, University of York, York, UK.
Correspondence e-mail: ez537@york.ac.uk

The subgroup structure of the hyperoctahedral group in six dimensions is investigated. In particular, the subgroups isomorphic to the icosahedral group are studied. The orthogonal crystallographic representations of the icosahedral group are classified and their intersections and subgroups analysed, using results from graph theory and their spectra.

1. Introduction

The discovery of quasicrystals in 1984 by Shechtman *et al.* has spurred the mathematical and physical community to develop mathematical tools in order to study structures with non-crystallographic symmetry.

Quasicrystals are alloys with five-, eight-, ten- and 12-fold symmetry in their atomic positions (Steurer, 2004), and therefore they cannot be organized as (periodic) lattices. In crystallographic terms, their symmetry group G is noncrystallographic. However, the noncrystallographic symmetry leaves a lattice invariant in higher dimensions, providing an integral representation of G . If such a representation is reducible and contains a two- or three-dimensional invariant subspace, then it is referred to as a crystallographic representation, following terminology given by Levitov & Rhyner (1988). This is the starting point to construct quasicrystals *via* the cut-and-project method described by, among others, Senechal (1995), or as a model set (Moody, 2000).

In this paper we are interested in icosahedral symmetry. The icosahedral group \mathcal{I} consists of all the rotations that leave a regular icosahedron invariant, it has size 60 and it is the largest of the finite subgroups of $SO(3)$. \mathcal{I} contains elements of order five, therefore it is noncrystallographic in three dimensions; the (minimal) crystallographic representation of it is six-dimensional (Levitov & Rhyner, 1988). The full icosahedral group, denoted by \mathcal{I}_h , also contains the reflections and is equal to $\mathcal{I} \times C_2$, where C_2 denotes the cyclic group of order two. \mathcal{I}_h is isomorphic to the Coxeter group H_3 (Humphreys, 1990) and is made up of 120 elements. In this work, we focus on the icosahedral group \mathcal{I} because it plays a central role in applications in virology (Indelicato *et al.*, 2011). However, our considerations apply equally to the larger group \mathcal{I}_h .

Levitov & Rhyner (1988) classified the Bravais lattices in \mathbb{R}^6 that are left invariant by \mathcal{I} : there are, up to equivalence, exactly three lattices, usually referred to as icosahedral Bravais lattices, namely the simple cubic (SC), body-centred cubic (BCC) and face-centred cubic (FCC). The point group of these lattices is the six-dimensional hyperoctahedral group,

denoted by B_6 , which is a subgroup of $O(6)$ and can be represented in the standard basis of \mathbb{R}^6 as the set of all 6×6 orthogonal and integral matrices. The subgroups of B_6 which are isomorphic to the icosahedral group constitute the integral representations of it; among them, the crystallographic ones are those which split, in $GL(6, \mathbb{R})$, into two three-dimensional irreducible representations of \mathcal{I} . Therefore, they carry two subspaces in \mathbb{R}^3 which are invariant under the action of \mathcal{I} and can be used to model the quasiperiodic structures.

The embedding of the icosahedral group into B_6 has been used extensively in the crystallographic literature. Katz (1989), Senechal (1995), Kramer & Zeidler (1989), Baake & Grimm (2013), among others, start from a six-dimensional crystallographic representation of \mathcal{I} to construct three-dimensional Penrose tilings and icosahedral quasicrystals. Kramer (1987) and Indelicato *et al.* (2011) also apply it to study structural transitions in quasicrystals. In particular, Kramer considers in B_6 a representation of \mathcal{I} and a representation of the octahedral group \mathcal{O} which share a tetrahedral subgroup, and defines a continuous rotation (called Schur rotation) between cubic and icosahedral symmetry which preserves intermediate tetrahedral symmetry. Indelicato *et al.* define a transition between two icosahedral lattices as a continuous path connecting the two lattice bases keeping some symmetry preserved, described by a maximal subgroup of the icosahedral group. The rationale behind this approach is that the two corresponding lattice groups share a common subgroup. These two approaches are shown to be related (Indelicato *et al.*, 2012), hence the idea is that it is possible to study the transitions between icosahedral quasicrystals by considering two distinct crystallographic representations of \mathcal{I} in B_6 which share a common subgroup.

These papers motivate the idea of studying in some detail the subgroup structure of B_6 . In particular, we focus on the subgroups isomorphic to the icosahedral group and its subgroups. Since the group is quite large (it has $2^6 6!$ elements), we use for computations the software *GAP* (The GAP Group, 2013), which is designed to compute properties of finite groups. More precisely, based on Baake (1984), we generate

the elements of B_6 in GAP as a subgroup of the symmetric group S_{12} and then find the classes of subgroups isomorphic to the icosahedral group. Among them we isolate, using results from character theory, the class of crystallographic representations of \mathcal{I} . In order to study the subgroup structure of this class, we propose a method using graph theory and their spectra. In particular, we treat the class of crystallographic representations of \mathcal{I} as a graph: we fix a subgroup \mathcal{G} of \mathcal{I} and say that two elements in the class are adjacent if their intersection is equal to a subgroup isomorphic to \mathcal{G} . We call the resulting graph \mathcal{G} -graph. These graphs are quite large and difficult to visualize; however, by analysing their spectra (Cvetkovic *et al.*, 1995) we can study in some detail their topology, hence describing the intersection and the subgroups shared by different representations.

The paper is organized as follows. After recalling, in §2, the definitions of point group and lattice group, we define, in §3, the crystallographic representations of the icosahedral group and the icosahedral lattices in six dimensions. We provide, following Kramer & Haase (1989), a method for the construction of the projection into three dimensions using tools from the representation theory of finite groups. In §4 we classify, with the help of GAP , the crystallographic representations of \mathcal{I} . In §5 we study their subgroup structure, introducing the concept of \mathcal{G} -graph, where \mathcal{G} is a subgroup of \mathcal{I} .

2. Lattices and noncrystallographic groups

Let $\mathbf{b}_i, i = 1, \dots, n$ be a basis of \mathbb{R}^n , and let $B \in GL(n, \mathbb{R})$ be the matrix whose columns are the components of \mathbf{b}_i with respect to the canonical basis $\{\mathbf{e}_i, i = 1, \dots, n\}$ of \mathbb{R}^n . A lattice in \mathbb{R}^n is a \mathbb{Z} -free module of rank n with basis B , *i.e.*

$$\mathcal{L}(B) = \left\{ \mathbf{x} = \sum_{i=1}^n m_i \mathbf{b}_i : m_i \in \mathbb{Z} \right\}.$$

Any other lattice basis is given by BM , where $M \in GL(n, \mathbb{Z})$, the set of invertible matrices with integral entries (whose determinant is equal to ± 1) (Artin, 1991).

The point group of a lattice \mathcal{L} is given by all the orthogonal transformations that leave the lattice invariant (Pitteri & Zanzotto, 2002):

$$\mathcal{P}(B) = \{Q \in O(n) : \exists M \in GL(n, \mathbb{Z}) \text{ s.t. } QB = BM\}.$$

We notice that, if $Q \in \mathcal{P}(B)$, then $B^{-1}QB = M \in GL(n, \mathbb{Z})$. In other words, the point group consists of all the orthogonal matrices which can be represented in the basis B as integral matrices. The set of all these matrices constitute the lattice group of the lattice:

$$\Lambda(B) = \{M \in GL(n, \mathbb{Z}) : \exists Q \in \mathcal{P}(B) \text{ s.t. } M = B^{-1}QB\}.$$

The lattice group provides an integral representation of the point group and these are related *via* the equation

$$\Lambda(B) = B^{-1}\mathcal{P}(B)B,$$

and moreover the following hold (Pitteri & Zanzotto, 2002):

Table 1
Character table of the icosahedral group.

Note that $\tau = (\sqrt{5} + 1)/2$ is the golden ratio.

Irrep	E	$12C_5$	$12C_5^2$	$15C_2$	$20C_3$
A	1	1	1	1	1
T_1	3	τ	$1-\tau$	-1	0
T_2	3	$1-\tau$	τ	-1	0
G	4	-1	-1	0	1
H	5	0	0	1	-1

$$\mathcal{P}(BM) = \mathcal{P}(B), \quad \Lambda(BM) = M^{-1}\Lambda(B)M, \quad M \in GL(n, \mathbb{Z}).$$

We notice that a change of basis in the lattice leaves the point group invariant, whereas the corresponding lattice groups are conjugated in $GL(n, \mathbb{Z})$. Two lattices are inequivalent if the corresponding lattice groups are not conjugated in $GL(n, \mathbb{Z})$ (Pitteri & Zanzotto, 2002).

As a consequence of the crystallographic restriction [see, for example, Baake & Grimm (2013)] five- and n -fold symmetries, where n is a natural number greater than six, are forbidden in dimensions two and three, and therefore any group G containing elements of such orders cannot be the point group of a two- or three-dimensional lattice. We therefore call these groups noncrystallographic. In particular, three-dimensional icosahedral lattices cannot exist. However, a noncrystallographic group leaves some lattices invariant in higher dimensions and the smallest such dimension is called the minimal embedding dimension. Following Levitov & Rhyner (1988), we introduce:

Definition 2.1. Let G be a noncrystallographic group. A crystallographic representation ρ of G is a D -dimensional representation of G such that:

- (1) the characters χ_ρ of ρ are integers;
- (2) ρ is reducible and contains a two- or three-dimensional representation of G .

We observe that the first condition implies that G must be the subgroup of the point group of a D -dimensional lattice. The second condition tells us that ρ contains either a two- or three-dimensional invariant subspace E of \mathbb{R}^D , usually referred to as physical space (Levitov & Rhyner, 1988).

3. Six-dimensional icosahedral lattices

The icosahedral group \mathcal{I} is generated by two elements, g_2 and g_3 , such that $g_2^2 = g_3^3 = (g_2g_3)^5 = e$, where e denotes the identity element. It has size 60 and it is isomorphic to A_5 , the alternating group of order five (Artin, 1991). Its character table is given in Table 1.

From the character table we see that the (minimal) crystallographic representation of \mathcal{I} is six-dimensional and is given by $T_1 \oplus T_2$. Therefore, \mathcal{I} leaves a lattice in \mathbb{R}^6 invariant. Levitov & Rhyner (1988) proved that the three inequivalent Bravais lattices of this type, mentioned in the *Introduction* and

referred to as icosahedral (Bravais) lattices, are given by, respectively:

$$\begin{aligned} \mathcal{L}_{\text{SC}} &= \{\mathbf{x} = (x_1, \dots, x_6) : x_i \in \mathbb{Z}\}, \\ \mathcal{L}_{\text{BCC}} &= \{\mathbf{x} = \frac{1}{2}(x_1, \dots, x_6) : x_i \in \mathbb{Z}, x_i = x_j \text{ mod } 2, \forall i, j = 1, \dots, 6\}, \\ \mathcal{L}_{\text{FCC}} &= \{\mathbf{x} = \frac{1}{2}(x_1, \dots, x_6) : x_i \in \mathbb{Z}, \sum_{i=1}^6 x_i = 0 \text{ mod } 2\}. \end{aligned}$$

We note that a basis of the SC lattice is the canonical basis of \mathbb{R}^6 . Its point group is given by

$$\mathcal{P}_{\text{SC}} = \{Q \in O(6) : Q = M \in GL(6, \mathbb{Z})\} = O(6) \cap GL(6, \mathbb{Z}) \simeq O(6, \mathbb{Z}), \quad (1)$$

which is the hyperoctahedral group in dimension six. In the following, we will denote this group by B_6 , following Humphreys (1996). We point out that this notation comes from Lie theory: indeed, B_6 represents the root system of the Lie algebra $\mathfrak{so}(13)$ (Fulton & Harris, 1991). However, the corresponding reflection group $W(B_6)$ is isomorphic to the hyperoctahedral group in six dimensions (Humphreys, 1990).

All three lattices have point group B_6 , whereas their lattice groups are different and, indeed, they are not conjugate in $GL(6, \mathbb{Z})$ (Levitov & Rhyner, 1988).

Let \mathcal{H} be a subgroup of B_6 isomorphic to \mathcal{I} . \mathcal{H} provides a (faithful) integral and orthogonal representation of \mathcal{I} . Moreover, if $\mathcal{H} \simeq T_1 \oplus T_2$ in $GL(6, \mathbb{R})$, then \mathcal{H} is also crystallographic (in the sense of Definition 2.1). All of the other crystallographic representations are given by $B^{-1}\mathcal{H}B$, where $B \in GL(6, \mathbb{R})$ is a basis of an icosahedral lattice in \mathbb{R}^6 . Therefore we can focus our attention, without loss of generality, on the orthogonal crystallographic representations.

3.1. Projection operators

Let \mathcal{H} be a crystallographic representation of the icosahedral group. \mathcal{H} splits into two three-dimensional irreducible representations (IRs), T_1 and T_2 , in $GL(6, \mathbb{R})$. This means that there exists a matrix $R \in GL(6, \mathbb{R})$ such that

$$\mathcal{H}' := R^{-1}\mathcal{H}R = \begin{pmatrix} T_1 & 0 \\ 0 & T_2 \end{pmatrix}. \quad (2)$$

The two IRs T_1 and T_2 leave two three-dimensional subspaces invariant, which are usually referred to as the physical (or parallel) space E^\parallel and the orthogonal space E^\perp (Katz, 1989). In order to find the matrix R (which is not unique in general), we follow (Kramer & Haase, 1989) and use results from the representation theory of finite groups (for proofs and further results see, for example, Fulton & Harris, 1991). In particular, let $\Gamma : G \rightarrow GL(n, F)$ be an n -dimensional representation of a finite group G over a field F ($F = \mathbb{R}, \mathbb{C}$). By Maschke's theorem, Γ splits, in $GL(n, F)$, as $m_1\Gamma_1 \oplus \dots \oplus m_r\Gamma_r$, where $\Gamma_i : G \rightarrow GL(n_i, F)$ is an n_i -dimensional IR of G . Then the projection operator $P_i : F^n \rightarrow F^{n_i}$ is given by

$$P_i := \frac{n_i}{|G|} \sum_{g \in \mathcal{I}} \chi_{\Gamma_i}^*(g)\Gamma(g), \quad (3)$$

where $\chi_{\Gamma_i}^*$ denotes the complex conjugate of the character of the representation Γ_i . This operator is such that its image

$\text{Im}(P_i)$ is equal to an n_i -dimensional subspace V_i of F^n invariant under Γ_i . In our case, we have two projection operators, $P_i : \mathbb{R}^6 \rightarrow \mathbb{R}^3$, $i = 1, 2$, corresponding to the IRs T_1 and T_2 , respectively. We assume the image of P_1 , $\text{Im}(P_1)$, to be equal to E^\parallel , and $\text{Im}(P_2) = E^\perp$. If $\{\mathbf{e}_j, j = 1, \dots, 6\}$ is the canonical basis of \mathbb{R}^6 , then a basis of E^\parallel (respectively E^\perp) can be found considering the set $\{\hat{\mathbf{e}}_j := P_i\mathbf{e}_j, j = 1, \dots, 6\}$ for $i = 1$ (respectively $i = 2$) and then extracting a basis \mathcal{B}_i from it. Since $\dim E^\parallel = \dim E^\perp = 3$, we obtain $\mathcal{B}_i = \{\hat{\mathbf{e}}_{i,1}, \hat{\mathbf{e}}_{i,2}, \hat{\mathbf{e}}_{i,3}\}$, for $i = 1, 2$. The matrix R can be thus written as

$$R = \begin{pmatrix} \hat{\mathbf{e}}_{1,1} & \hat{\mathbf{e}}_{1,2} & \hat{\mathbf{e}}_{1,3} & \hat{\mathbf{e}}_{2,1} & \hat{\mathbf{e}}_{2,2} & \hat{\mathbf{e}}_{2,3} \end{pmatrix}. \quad (4)$$

basis of E^\parallel
basis of E^\perp

Denoting by π^\parallel and π^\perp the 3×6 matrices which represent P_1 and P_2 in the bases \mathcal{B}_1 and \mathcal{B}_2 , respectively, we have, by linear algebra

$$R^{-1} = \begin{pmatrix} \pi^\parallel \\ \pi^\perp \end{pmatrix}. \quad (5)$$

Since $R^{-1}\mathcal{H} = \mathcal{H}'R^{-1}$ [cf. equation (2)], we obtain

$$\pi^\parallel(\mathcal{H}(g)\mathbf{v}) = T_1(\pi^\parallel(\mathbf{v})), \quad \pi^\perp(\mathcal{H}(g)\mathbf{v}) = T_2(\pi^\perp(\mathbf{v})), \quad (6)$$

for all $g \in \mathcal{I}$ and $\mathbf{v} \in \mathbb{R}^6$. In particular, the following diagram commutes

$$\begin{array}{ccc} \mathbb{R}^6 & \xrightarrow{\mathcal{H}} & \mathbb{R}^6 \\ \downarrow \pi^\parallel & & \downarrow \pi^\parallel \\ E^\parallel & \xrightarrow{T_1} & E^\parallel \end{array} \quad (7)$$

The set $(\mathcal{H}, \pi^\parallel)$ is the starting point for the construction of quasicrystals via the cut-and-project method (Senechal, 1995; Indelicato *et al.*, 2012).

4. Crystallographic representations of \mathcal{I}

From the previous section it follows that the six-dimensional hyperoctahedral group B_6 contains all the (minimal) orthogonal crystallographic representations of the icosahedral group. In this section we classify them, with the help of the computer software programme GAP (The GAP Group, 2013).

4.1. Representations of the hyperoctahedral group B_6

Permutation representations of the n -dimensional hyperoctahedral group B_n in terms of elements of S_{2n} , the symmetric group of order $2n$, have been described by Baake (1984). In this subsection, we review these results because they allow us to generate B_6 in GAP and further study its subgroup structure.

It follows from equation (1) that B_6 consists of all the orthogonal integral matrices. A matrix $A = (a_{ij})$ of this kind must satisfy $AA^T = I_6$, the identity matrix of order six, and have integral entries only. It is easy to see that these conditions imply that A has entries in $\{0, \pm 1\}$ and each row and column contains 1 or -1 only once. These matrices are called signed

permutation matrices. It is straightforward to see that any $A \in B_6$ can be written in the form NQ , where Q is a 6×6 permutation matrix and N is a diagonal matrix with each diagonal entry being either 1 or -1 . We can thus associate with each matrix in B_6 a pair (\mathbf{a}, π) , where $\mathbf{a} \in \mathbb{Z}_2^6$ is a vector given by the diagonal elements of N , and $\pi \in S_6$ is the permutation associated with Q . The set of all these pairs constitutes a group (called the wreath product of \mathbb{Z}_2 and S_6 , and denoted by $\mathbb{Z}_2 \wr S_6$; Humphreys, 1996) with the multiplication rule given by

$$(\mathbf{a}, \pi)(\mathbf{b}, \sigma) := (\mathbf{a}_\sigma +_2 \mathbf{b}, \pi\sigma),$$

where $+_2$ denotes addition modulo 2 and

$$(\mathbf{a}_\sigma)_k := a_{\sigma(k)}, \quad \mathbf{a} = (a_1, \dots, a_6).$$

$\mathbb{Z}_2 \wr S_6$ and B_6 are isomorphic, an isomorphism T being the following:

$$[T(\mathbf{a}, \pi)]_{ij} := (-1)^{a_i} \delta_{\pi(i),j}. \tag{8}$$

It immediately follows that $|B_6| = 2^6 6! = 46\,080$. A set of generators is given by

$$\alpha := (\mathbf{0}, (1, 2)), \beta := (\mathbf{0}, (1, 2, 3, 4, 5, 6)), \gamma := ((0, 0, 0, 0, 0, 1), \text{id}_{S_6}), \tag{9}$$

which satisfy the relations

$$\alpha^2 = \gamma^2 = \beta^6 = (\mathbf{0}, \text{id}_{S_6}).$$

Finally, the function $\varphi : \mathbb{Z}_2 \wr S_6 \rightarrow S_{12}$ defined by

$$\varphi(\mathbf{a}, \pi)(k) := \begin{cases} \pi(k) + 6a_k & \text{if } 1 \leq k \leq 6 \\ \pi(k - 6) + 6(1 - a_{k-6}) & \text{if } 7 \leq k \leq 12 \end{cases} \tag{10}$$

is injective and maps any element of $\mathbb{Z}_2 \wr S_6$ into a permutation of S_{12} , and provides a faithful permutation representation of B_6 as a subgroup of S_{12} . Combining equation (8) with the inverse of equation (10) we get the function

$$\psi := T \circ \varphi^{-1} : S_{12} \rightarrow B_6, \tag{11}$$

which can be used to map a permutation into an element of B_6 .

4.2. Classification

In this subsection we classify the orthogonal crystallographic representations of the icosahedral group. We start by recalling a standard way to construct such a representation, following Zappa *et al.* (2013). We consider a regular icosahedron and we label each vertex by a number from one to 12, so that the vertex opposite to vertex i is labelled by $i + 6$ (see Fig. 1). This labelling induces a permutation representation $\sigma : \mathcal{I} \rightarrow S_{12}$ given by

$$\begin{aligned} \sigma(g_2) &= (1, 6)(2, 5)(3, 9)(4, 10)(7, 12)(8, 11), \\ \sigma(g_3) &= (1, 5, 6)(2, 9, 4)(7, 11, 12)(3, 10, 8). \end{aligned}$$

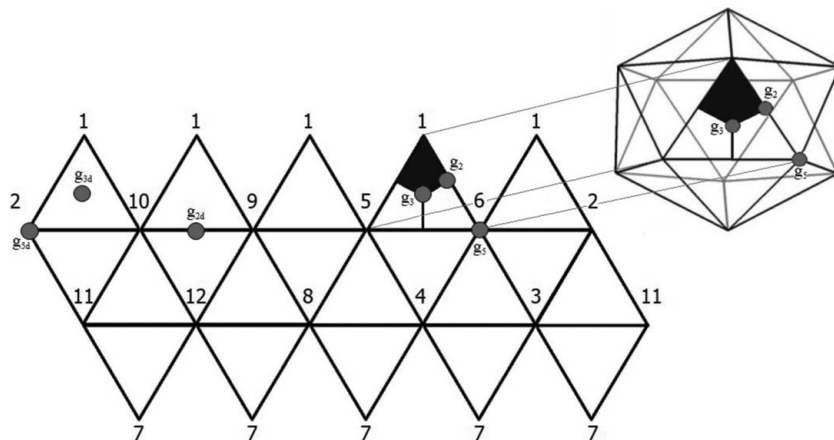


Figure 1

A planar representation of an icosahedral surface, showing our labelling convention for the vertices; the dots represent the locations of the symmetry axes corresponding to the generators of the icosahedral group and its subgroups. The kite highlighted is a fundamental domain of the icosahedral group.

Using equation (11) we obtain a representation $\hat{\mathcal{I}} : \mathcal{I} \rightarrow B_6$ given by

$$\hat{\mathcal{I}}(g_2) = \begin{pmatrix} 0 & 0 & 0 & 0 & 0 & 1 \\ 0 & 0 & 0 & 0 & 1 & 0 \\ 0 & 0 & -1 & 0 & 0 & 0 \\ 0 & 0 & 0 & -1 & 0 & 0 \\ 0 & 1 & 0 & 0 & 0 & 0 \\ 1 & 0 & 0 & 0 & 0 & 0 \end{pmatrix}, \quad \hat{\mathcal{I}}(g_3) = \begin{pmatrix} 0 & 0 & 0 & 0 & 0 & 1 \\ 0 & 0 & 0 & 1 & 0 & 0 \\ 0 & -1 & 0 & 0 & 0 & 0 \\ 0 & 0 & -1 & 0 & 0 & 0 \\ 1 & 0 & 0 & 0 & 0 & 0 \\ 0 & 0 & 0 & 0 & 1 & 0 \end{pmatrix}. \tag{12}$$

We see that $\chi_{\hat{\mathcal{I}}}(g_2) = -2$ and $\chi_{\hat{\mathcal{I}}}(g_3) = 0$, so that, by looking at the character table of \mathcal{I} , we have

$$\chi_{\hat{\mathcal{I}}} = \chi_{T_1} + \chi_{T_2},$$

which implies, using Maschke's theorem (Fulton & Harris, 1991), that $\hat{\mathcal{I}} \simeq T_1 \oplus T_2$ in $GL(6, \mathbb{R})$. Therefore, the subgroup $\hat{\mathcal{I}}$ of B_6 is a crystallographic representation of \mathcal{I} .

Before we continue, we recall the following (Humphreys, 1996):

Definition 4.1. Let H be a subgroup of a group G . The conjugacy class of H in G is the set

$$\mathcal{C}_G(H) := \{gHg^{-1} : g \in G\}.$$

In order to find all the other crystallographic representations, we use the following scheme:

(a) we generate B_6 as a subgroup of S_{12} using equations (9) and (10);

(b) we list all the conjugacy classes of the subgroups of B_6 and find a representative for each class;

(c) we isolate the classes whose representatives have order 60;

(d) we check if these representatives are isomorphic to \mathcal{I} ;

(e) we map these subgroups of S_{12} into B_6 using equation (11) and isolate the crystallographic ones by checking the characters; denoting by S the representative, we decompose χ_S as

$$\chi_S = m_1\chi_A + m_2\chi_{T_1} + m_3\chi_{T_2} + m_4\chi_G + m_5\chi_H,$$

$$m_i \in \mathbb{N}, i = 1, \dots, 5.$$

Note that S is crystallographic if and only if $m_2 = m_3 = 1$ and $m_1 = m_4 = m_5 = 0$.

We implemented steps (1)–(4) in *GAP* (see Appendix C). There are three conjugacy classes of subgroups isomorphic to \mathcal{I} in B_6 . Denoting by $S_i = \langle g_{2,i}, g_{3,i} \rangle$ the representatives of the classes returned by *GAP*, we have, using equation (11),

$$\chi_{S_1}(g_{2,1}) = 2, \chi_{S_1}(g_{3,1}) = 3 \Rightarrow \chi_{S_1} = 2\chi_A + \chi_G \Rightarrow S_1 \simeq 2A \oplus G,$$

$$\chi_{S_2}(g_{2,2}) = -2, \chi_{S_2}(g_{3,2}) = 0 \Rightarrow \chi_{S_2} = \chi_{T_1} + \chi_{T_2} \Rightarrow S_2 \simeq T_1 \oplus T_2,$$

$$\chi_{S_3}(g_{2,3}) = 2, \chi_{S_3}(g_{3,3}) = 0 \Rightarrow \chi_{S_3} = \chi_A + \chi_H \Rightarrow S_3 \simeq A \oplus H.$$

Since $2A$ is decomposable into two one-dimensional representations, it is not strictly speaking two dimensional in the sense of Definition 2.1, and as a consequence, only the second class contains the crystallographic representations of \mathcal{I} . A computation in *GAP* shows that its size is 192. We thus have the following:

Proposition 4.1. The crystallographic representations of \mathcal{I} in B_6 form a unique conjugacy class in the set of all the classes of subgroups of B_6 , and its size is equal to 192.

We briefly point out that the other two classes of subgroups isomorphic to \mathcal{I} in B_6 have an interesting algebraic interpretation. First of all, we observe that B_6 is an extension of S_6 , since according to Humphreys (1996):

$$B_6/\mathbb{Z}_2^6 \simeq (\mathbb{Z}_2 \wr S_6)/\mathbb{Z}_2^6 \simeq S_6.$$

Following Janusz & Rotman (1982), it is possible to embed the symmetric group S_5 into S_6 in two different ways. The canonical embedding is achieved by fixing a point in $\{1, \dots, 6\}$ and permuting the other five, whereas the other embedding is by means of the so-called ‘exotic map’ $\varphi : S_5 \rightarrow S_6$, which acts on the six 5-Sylow subgroups of S_5 by conjugation. Recalling that the icosahedral group is isomorphic to the alternating group A_5 , which is a normal subgroup of S_5 , then the canonical embedding corresponds to the representation $2A \oplus G$ in B_6 , while the exotic one corresponds to the representation $A \oplus H$.

In what follows, we will consider the subgroup $\hat{\mathcal{I}}$ previously defined as a representative of the class of the crystallographic representations of \mathcal{I} , and denote this class by $\mathcal{C}_{B_6}(\hat{\mathcal{I}})$.

Recalling that two representations $D^{(1)}$ and $D^{(2)}$ of a group G are said to be equivalent if there are related *via* a similarity transformation, *i.e.* there exists an invertible matrix S such that

$$D^{(1)} = SD^{(2)}S^{-1},$$

then an immediate consequence of Proposition 4.1 is the following:

Corollary 4.1. Let \mathcal{H}_1 and \mathcal{H}_2 be two orthogonal crystallographic representations of \mathcal{I} . Then \mathcal{H}_1 and \mathcal{H}_2 are equivalent in B_6 .

We observe that the determinant of the generators of $\hat{\mathcal{I}}$ in equation (12) is equal to one, so that $\hat{\mathcal{I}} \in B_6^+ := \{A \in B_6 : \det A = 1\}$. Proposition 4.1 implies that all the crystallographic representations belong to B_6^+ . The remark-

able fact is that they split into two different classes in B_6^+ . To see this, we first need to generate B_6^+ . In particular, with *GAP* we isolate the subgroups of index two in B_6 , which are normal in B_6 , and then, using equation (11), we find the one whose generators have determinant equal to one. In particular, we have

$$B_6^+ = \langle (1, 2, 6, 4, 3)(7, 8, 12, 10, 9), (5, 11)(6, 12), \\ (1, 2, 6, 5, 3)(7, 8, 12, 11, 9), (5, 12, 11, 6) \rangle.$$

We can then apply the same procedure to find the crystallographic representations of \mathcal{I} , and see that they split into two classes, each one of size 96. Again we can choose $\hat{\mathcal{I}}$ as a representative for one of these classes; a representative $\hat{\mathcal{K}}$ for the other one is given by

$$\hat{\mathcal{K}} = \left\langle \begin{pmatrix} 0 & 1 & 0 & 0 & 0 & 0 \\ 1 & 0 & 0 & 0 & 0 & 0 \\ 0 & 0 & -1 & 0 & 0 & 0 \\ 0 & 0 & 0 & 0 & 0 & 1 \\ 0 & 0 & 0 & 0 & -1 & 0 \\ 0 & 0 & 0 & 1 & 0 & 0 \end{pmatrix}, \begin{pmatrix} 0 & 0 & 0 & 1 & 0 & 0 \\ 1 & 0 & 0 & 0 & 0 & 0 \\ 0 & 0 & 0 & 0 & 0 & -1 \\ 0 & 1 & 0 & 0 & 0 & 0 \\ 0 & 0 & -1 & 0 & 0 & 0 \\ 0 & 0 & 0 & 0 & 1 & 0 \end{pmatrix} \right\rangle. \tag{13}$$

We note that in the more general case of \mathcal{I}_h , we can construct the crystallographic representations of \mathcal{I}_h starting from the crystallographic representations of \mathcal{I} . First of all, we recall that $\mathcal{I}_h = I \times C_2$, where C_2 is the cyclic group of order two. Let \mathcal{H} be a crystallographic representation of \mathcal{I} in B_6 , and let $\Gamma = \{1, -1\}$ be a one-dimensional representation of C_2 . Then the representation $\hat{\mathcal{H}}$ given by

$$\hat{\mathcal{H}} := \mathcal{H} \otimes \Gamma,$$

where \otimes denotes the tensor product of matrices, is a representation of \mathcal{I}_h in B_6 and it is crystallographic in the sense of Definition 2.1 (Fulton & Harris, 1991).

4.3. Projection into the three-dimensional space

We study in detail the projection into the physical space E^{\parallel} using the methods described in §3.1.

Let $\hat{\mathcal{I}}$ be the crystallographic representation of \mathcal{I} given in equation (12). Using equation (3) with $n_i = 3$ and $|G| = |\mathcal{I}| = 60$ we obtain the following projection operators

$$P_1 = \frac{1}{2\sqrt{5}} \begin{pmatrix} \sqrt{5} & 1 & -1 & -1 & 1 & 1 \\ 1 & \sqrt{5} & 1 & -1 & -1 & 1 \\ -1 & 1 & \sqrt{5} & 1 & -1 & 1 \\ -1 & -1 & 1 & \sqrt{5} & 1 & 1 \\ 1 & -1 & -1 & 1 & \sqrt{5} & 1 \\ 1 & 1 & 1 & 1 & 1 & \sqrt{5} \end{pmatrix},$$

$$P_2 = \frac{1}{2\sqrt{5}} \begin{pmatrix} \sqrt{5} & -1 & 1 & 1 & -1 & -1 \\ -1 & \sqrt{5} & -1 & 1 & 1 & -1 \\ 1 & -1 & \sqrt{5} & -1 & 1 & -1 \\ 1 & 1 & -1 & \sqrt{5} & -1 & -1 \\ -1 & 1 & 1 & -1 & \sqrt{5} & -1 \\ -1 & -1 & -1 & -1 & -1 & \sqrt{5} \end{pmatrix}.$$

Table 2

Explicit forms of the IRs T_1 and T_2 with $\hat{\mathcal{I}} \simeq T_1 \oplus T_2$.

Generator	Irrep T_1	Irrep T_2
g_2	$\frac{1}{2} \begin{pmatrix} \tau-1 & 1 & \tau \\ 1 & -\tau & \tau-1 \\ \tau & \tau-1 & -1 \end{pmatrix}$	$\frac{1}{2} \begin{pmatrix} \tau-1 & -\tau & -1 \\ -\tau & -1 & \tau-1 \\ -1 & \tau-1 & -\tau \end{pmatrix}$
g_3	$\frac{1}{2} \begin{pmatrix} \tau & \tau-1 & 1 \\ 1-\tau & -1 & \tau \\ 1 & -\tau & 1-\tau \end{pmatrix}$	$\frac{1}{2} \begin{pmatrix} -1 & 1-\tau & -\tau \\ \tau-1 & \tau & -1 \\ \tau & -1 & 1-\tau \end{pmatrix}$

Table 3

Nontrivial subgroups of the icosahedral group.

\mathcal{T} stands for the tetrahedral group, \mathcal{D}_{2n} for the dihedral group of size $2n$, and C_n for the cyclic group of size n .

Subgroup	Generators	Relations	Size
\mathcal{T}	g_2, g_{3d}	$g_2^2 = g_{3d}^3 = (g_2 g_{3d})^3 = e$	12
\mathcal{D}_{10}	g_{2d}, g_{5d}	$g_{2d}^2 = g_{5d}^5 = (g_{5d} g_{2d})^2 = e$	10
\mathcal{D}_6	g_{2d}, g_3	$g_{2d}^2 = g_3^3 = (g_3 g_{2d})^2 = e$	6
C_5	g_{5d}	$g_{5d}^5 = e$	5
\mathcal{D}_4	g_{2d}, g_2	$g_{2d}^2 = g_2^2 = (g_2 g_{2d})^2 = e$	4
C_3	g_3	$g_3^3 = e$	3
C_2	g_2	$g_2^2 = e$	2

The rank of these operators is equal to three. We choose as a basis of E^\parallel and E^\perp the following linear combination of the columns $\mathbf{c}_{i,j}$ of the projection operators P_i , for $i = 1, 2$ and $j = 1, \dots, 6$:

$$\left(\underbrace{\frac{\mathbf{c}_{1,1} + \mathbf{c}_{1,5}}{2}, \frac{\mathbf{c}_{1,2} - \mathbf{c}_{1,4}}{2}, \frac{\mathbf{c}_{1,3} + \mathbf{c}_{1,6}}{2}}_{\text{basis of } E^\parallel}, \underbrace{\frac{\mathbf{c}_{2,1} - \mathbf{c}_{2,5}}{2}, \frac{\mathbf{c}_{2,2} + \mathbf{c}_{2,4}}{2}, \frac{\mathbf{c}_{2,3} - \mathbf{c}_{2,6}}{2}}_{\text{basis of } E^\perp} \right).$$

With a suitable rescaling, we obtain the matrix R given by

$$R = \frac{1}{\sqrt{2(2+\tau)}} \begin{pmatrix} \tau & 1 & 0 & \tau & 0 & 1 \\ 0 & \tau & 1 & -1 & \tau & 0 \\ -1 & 0 & \tau & 0 & -1 & \tau \\ 0 & -\tau & 1 & 1 & \tau & 0 \\ \tau & -1 & 0 & -\tau & 0 & 1 \\ 1 & 0 & \tau & 0 & -1 & -\tau \end{pmatrix}.$$

The matrix R is orthogonal and reduces $\hat{\mathcal{I}}$ as in equation (2). In Table 2 we give the explicit forms of the reduced representation. The matrix representation in E^\parallel of P_1 is given by [see equation (5)]

$$\pi^\parallel = \frac{1}{\sqrt{2(2+\tau)}} \begin{pmatrix} \tau & 0 & -1 & 0 & \tau & 1 \\ 1 & \tau & 0 & -\tau & -1 & 0 \\ 0 & 1 & \tau & 1 & 0 & \tau \end{pmatrix}.$$

The orbit $\{T_1(\pi^\parallel(\mathbf{e}_j))\}$, where $\{\mathbf{e}_j, j = 1, \dots, 6\}$ is the canonical basis of \mathbb{R}^6 , represents a regular icosahedron in three

Table 4

Permutation representations of the generators of the subgroups of the icosahedral group.

$\sigma(g_2) = (1, 6)(2, 5)(3, 9)(4, 10)(7, 12)(8, 11)$
$\sigma(g_{2d}) = (1, 12)(2, 8)(3, 4)(5, 11)(6, 7)(9, 10)$
$\sigma(g_3) = (1, 5, 6)(2, 9, 4)(7, 11, 12)(3, 10, 8)$
$\sigma(g_{3d}) = (1, 10, 2)(3, 5, 12)(4, 8, 7)(6, 9, 11)$
$\sigma(g_5) = (1, 2, 3, 4, 5)(7, 8, 9, 10, 11)$
$\sigma(g_{5d}) = (1, 10, 11, 3, 6)(4, 5, 9, 12, 7)$

Table 5

Sizes of the classes of subgroups of the icosahedral group in \mathcal{I} and B_6 .

Subgroup	$ \mathcal{C}_{\mathcal{I}}(\mathcal{G}) $	$ \mathcal{C}_{B_6}(\mathcal{K}_{\mathcal{G}}) $
\mathcal{I}	5	480
\mathcal{D}_{10}	6	576
\mathcal{D}_6	10	960
\mathcal{D}_4	5	120
C_5	6	576
C_3	10	320
C_2	15	180

dimensions centred at the origin (Senechal, 1995; Katz, 1989; Indelicato *et al.*, 2011).

Let \mathcal{K} be another crystallographic representation of \mathcal{I} in B_6 . By Proposition 4.1, \mathcal{K} and $\hat{\mathcal{I}}$ are conjugated in B_6 . Consider $M \in B_6$ such that $M\hat{\mathcal{I}}M^{-1} = \mathcal{K}$ and let $S = MR$. We have

$$S^{-1}\mathcal{K}S = (MR)^{-1}\mathcal{K}(MR) = R^{-1}M^{-1}\mathcal{K}MR = R^{-1}\hat{\mathcal{I}}R = T_1 \oplus T_2.$$

Therefore it is possible, with a suitable choice of the reducing matrices, to project all the crystallographic representations of \mathcal{I} in B_6 in the same physical space.

5. Subgroup structure

The nontrivial subgroups of \mathcal{I} are listed in Table 3, together with their generators (Hoyle, 2004). Note that \mathcal{T} , \mathcal{D}_{10} and \mathcal{D}_6 are maximal subgroups of \mathcal{I} , and that \mathcal{D}_4 , C_5 and C_3 are normal subgroups of \mathcal{T} , \mathcal{D}_{10} and \mathcal{D}_6 , respectively (Humphreys, 1996; Artin, 1991). The permutation representations of the generators in S_{12} are given in Table 4 (see also Fig. 1).

Since \mathcal{I} is a small group, its subgroup structure can be easily obtained in *GAP* by computing explicitly all its conjugacy classes of subgroups. In particular, there are seven classes of nontrivial subgroups in \mathcal{I} : any subgroup H of \mathcal{I} has the property that, if K is another subgroup of \mathcal{I} isomorphic to H , then H and K are conjugate in \mathcal{I} (this property is referred to as the ‘friendliness’ of the subgroup H ; Soicher, 2006). In other words, denoting by $n_{\mathcal{G}}$ the number of subgroups of \mathcal{I} isomorphic to \mathcal{G} , *i.e.*

$$n_{\mathcal{G}} := |\{H < \mathcal{I} : H \simeq \mathcal{G}\}|, \tag{14}$$

we have (*cf.* Definition 4.1)

$$n_{\mathcal{G}} = |\mathcal{C}_{\mathcal{I}}(\mathcal{G})|.$$

In Table 5 we list the size of each class of subgroups in \mathcal{I} . Geometrically, different copies of C_2 , C_3 and C_5 correspond to the different two-, three- and fivefold axes of the icosahedron, respectively. In particular, different copies of \mathcal{D}_{10} stabilize one

of the six fivefold axes of the icosahedron, and each copy of \mathcal{D}_6 stabilizes one of the ten threefold axes. Moreover, it is possible to inscribe five tetrahedra into a dodecahedron, and each different copy of the tetrahedral group in \mathcal{I} stabilizes one of these tetrahedra.

5.1. Subgroups of the crystallographic representations of \mathcal{I}

Let \mathcal{G} be a subgroup of \mathcal{I} . The function (11) provides a representation of \mathcal{G} in B_6 , denoted by $\mathcal{K}_{\mathcal{G}}$, which is a subgroup of $\hat{\mathcal{I}}$. Let us denote by $\mathcal{C}_{B_6}(\mathcal{K}_{\mathcal{G}})$ the conjugacy class of $\mathcal{K}_{\mathcal{G}}$ in B_6 . The next lemma shows that this class contains all the subgroups of the crystallographic representations of \mathcal{I} in B_6 .

Lemma 5.1. Let $\mathcal{H}_i \in \mathcal{C}_{B_6}(\hat{\mathcal{I}})$ be a crystallographic representation of \mathcal{I} in B_6 and let $\mathcal{K}_i \subseteq \mathcal{H}_i$ be a subgroup of \mathcal{H}_i isomorphic to \mathcal{G} . Then $\mathcal{K}_i \in \mathcal{C}_{B_6}(\mathcal{K}_{\mathcal{G}})$.

Proof. Since $\mathcal{H}_i \in \mathcal{C}_{B_6}(\hat{\mathcal{I}})$, there exists $g \in B_6$ such that $g\mathcal{H}_i g^{-1} = \hat{\mathcal{I}}$, and therefore $g\mathcal{K}_i g^{-1} = \mathcal{K}'$ is a subgroup of $\hat{\mathcal{I}}$ isomorphic to \mathcal{G} . Since all these subgroups are conjugate in $\hat{\mathcal{I}}$ [they are ‘friendly’ in the sense intended by Soicher (2006)], there exists $h \in \hat{\mathcal{I}}$ such that $h\mathcal{K}'h^{-1} = \mathcal{K}_{\mathcal{G}}$. Thus $(hg)\mathcal{K}_i(hg)^{-1} = \mathcal{K}_{\mathcal{G}}$, implying that $\mathcal{K}_i \in \mathcal{C}_{B_6}(\mathcal{K}_{\mathcal{G}})$. \square

We next show that every element of $\mathcal{C}_{B_6}(\mathcal{K}_{\mathcal{G}})$ is a subgroup of a crystallographic representation of \mathcal{I} .

Lemma 5.2. Let $\mathcal{K}_i \in \mathcal{C}_{B_6}(\mathcal{K}_{\mathcal{G}})$. There exists $\mathcal{H}_i \in \mathcal{C}_{B_6}(\hat{\mathcal{I}})$ such that \mathcal{K}_i is a subgroup of \mathcal{H}_i .

Proof. Since $\mathcal{K}_i \in \mathcal{C}_{B_6}(\mathcal{K}_{\mathcal{G}})$, there exists $g \in B_6$ such that $g\mathcal{K}_i g^{-1} = \mathcal{K}_{\mathcal{G}}$. We define $\mathcal{H}_i := g^{-1}\hat{\mathcal{I}}g$. It can be seen immediately that \mathcal{K}_i is a subgroup of \mathcal{H}_i . \square

As a consequence of these lemmata, $\mathcal{C}_{B_6}(\mathcal{K}_{\mathcal{G}})$ contains all the subgroups of B_6 which are isomorphic to \mathcal{G} and are subgroups of a crystallographic representation of \mathcal{I} . The explicit forms of $\mathcal{K}_{\mathcal{G}}$ are given in Appendix B. We point out that it is possible to find subgroups of B_6 isomorphic to a subgroup \mathcal{G} of \mathcal{I} which are not subgroups of any crystallographic representation of \mathcal{I} . For example, the following subgroup

$$\hat{\mathcal{T}} = \left\langle \begin{pmatrix} 1 & 0 & 0 & 0 & 0 & 0 \\ 0 & -1 & 0 & 0 & 0 & 0 \\ 0 & 0 & -1 & 0 & 0 & 0 \\ 0 & 0 & 0 & -1 & 0 & 0 \\ 0 & 0 & 0 & 0 & -1 & 0 \\ 0 & 0 & 0 & 0 & 0 & 1 \end{pmatrix}, \begin{pmatrix} 0 & 0 & -1 & 0 & 0 & 0 \\ 1 & 0 & 0 & 0 & 0 & 0 \\ 0 & -1 & 0 & 0 & 0 & 0 \\ 0 & 0 & 0 & 0 & 0 & 1 \\ 0 & 0 & 0 & 1 & 0 & 0 \\ 0 & 0 & 0 & 0 & 1 & 0 \end{pmatrix} \right\rangle$$

is isomorphic to the tetrahedral group \mathcal{T} ; a computation in GAP shows that it is not a subgroup of any elements in $\mathcal{C}_{B_6}(\hat{\mathcal{I}})$. Indeed, the two classes of subgroups, $\mathcal{C}_{B_6}(\mathcal{K}_{\mathcal{T}})$ and $\mathcal{C}_{B_6}(\hat{\mathcal{T}})$, are disjoint.

Using GAP, we compute the size of each $\mathcal{C}_{B_6}(\mathcal{K}_{\mathcal{G}})$ (see Table 5). We observe that $|\mathcal{C}_{B_6}(\mathcal{K}_{\mathcal{G}})| < |\mathcal{C}_{B_6}(\hat{\mathcal{I}})| \cdot n_{\mathcal{G}}$. This implies that

crystallographic representations of \mathcal{I} may share subgroups. In order to describe more precisely the subgroup structure of $\mathcal{C}_{B_6}(\hat{\mathcal{I}})$ we will use some basic results from graph theory and their spectra, which we are going to recall in the next section.

5.2. Some basic results of graph theory and their spectra

In this section we recall, without proofs, some concepts and results from graph theory and spectral graph theory. Proofs and further results can be found, for example, in Foulds (1992) and Cvetkovic *et al.* (1995).

Let G be a graph with vertex set $V = \{v_1, \dots, v_n\}$. The number of edges incident with a vertex v is called the degree of v . If all vertices have the same degree d , then the graph is called regular of degree d . A walk of length l is a sequence of l consecutive edges and it is called a path if they are all distinct. A circuit is a path starting and ending at the same vertex and the girth of the graph is the length of the shortest circuit. Two vertices p and q are connected if there exists a path containing p and q . The connected component of a vertex v is the set of all vertices connected to v .

The adjacency matrix A of G is the $n \times n$ matrix $A = (a_{ij})$ whose entries a_{ij} are equal to one if the vertex v_i is adjacent to the vertex v_j , and zero otherwise. It can be seen immediately from its definition that A is symmetric and $a_{ii} = 0$ for all i , so that $\text{Tr}(A) = 0$. It follows that A is diagonalisable and all its eigenvalues are real. The spectrum of the graph is the set of all the eigenvalues of its adjacency matrix A , usually denoted by $\sigma(A)$.

Theorem 5.1. Let A be the adjacency matrix of a graph G with vertex set $V = \{v_1, \dots, v_n\}$. Let $N_k(i, j)$ denote the number of walks of length k starting at vertex v_i and finishing at vertex v_j . We have

$$N_k(i, j) = A_{ij}^k.$$

We recall that the spectral radius of a matrix A is defined by $\rho(A) := \max\{|\lambda| : \lambda \in \sigma(A)\}$. If A is a non-negative matrix, *i.e.* if all its entries are non-negative, then $\rho(A) \in \sigma(A)$ (Horn & Johnson, 1985). Since the adjacency matrix of a graph is non-negative, $|\lambda| \leq \rho(A) := r$, where $\lambda \in \sigma(A)$ and r is the largest eigenvalue. r is called the index of the graph G .

Theorem 5.2. Let $\lambda_1, \dots, \lambda_n$ be the spectrum of a graph G , and let r denote its index. Then G is regular of degree r if and only if

$$\frac{1}{n} \sum_{i=1}^n \lambda_i^2 = r.$$

Moreover, if G is regular the multiplicity of its index is equal to the number of its connected components.

5.3. Applications to the subgroup structure

Let \mathcal{G} be a subgroup of \mathcal{I} . In the following we represent the subgroup structure of the class of crystallographic representations of \mathcal{I} in B_6 , $\mathcal{C}_{B_6}(\hat{\mathcal{I}})$, as a graph. We say that

$\mathcal{H}_1, \mathcal{H}_2 \in \mathcal{C}_{B_6}(\hat{\mathcal{I}})$ are adjacent to each other (i.e. connected by an edge) in the graph if there exists $P \in \mathcal{C}_{B_6}(\mathcal{K}_G)$ such that $P = \mathcal{H}_1 \cap \mathcal{H}_2$. We can therefore consider the graph $G = (\mathcal{C}_{B_6}(\hat{\mathcal{I}}), E)$, where an edge $e \in E$ is of the form $(\mathcal{H}_1, \mathcal{H}_2)$. We call this graph \mathcal{G} -graph.

Using *GAP*, we compute the adjacency matrices of the \mathcal{G} -graphs. The algorithms used are shown in Appendix C. The spectra of the \mathcal{G} -graphs are given in Table 6. We first of all notice that the adjacency matrix of the C_5 -graph is the null matrix, implying that there are no two representations sharing precisely a subgroup isomorphic to C_5 , i.e. not a subgroup containing C_5 . We point out that, since the adjacency matrix of the \mathcal{D}_{10} -graph is not the null one, then there exist crystallographic representations, say \mathcal{H}_i and \mathcal{H}_j , sharing a maximal subgroup isomorphic to \mathcal{D}_{10} . Since C_5 is a (normal) subgroup of \mathcal{D}_{10} , then \mathcal{H}_i and \mathcal{H}_j do share a C_5 subgroup, but also a C_2 subgroup. In other words, if two representations share a fivefold axis, then necessarily they also share a twofold axis.

A straightforward calculation based on Theorem 5.2 leads to the following

Proposition 5.1. Let \mathcal{G} be a subgroup of \mathcal{I} . Then the corresponding \mathcal{G} -graph is regular.

In particular, the degree $d_{\mathcal{G}}$ of each \mathcal{G} -graph is equal to the largest eigenvalue of the corresponding spectrum. As a consequence we have the following:

Proposition 5.2. Let \mathcal{H} be a crystallographic representation of \mathcal{I} in B_6 . Then there are exactly $d_{\mathcal{G}}$ representations $\mathcal{K}_j \in \mathcal{C}_{B_6}(\hat{\mathcal{I}})$ such that

$$\mathcal{H} \cap \mathcal{K}_j = P_j, \exists P_j \in \mathcal{C}(\mathcal{K}_G), j = 1, \dots, d_{\mathcal{G}}.$$

In particular, we have $d_{\mathcal{G}} = 5, 6, 10, 0, 30, 20, 60$ and 60 for $\mathcal{G} = \mathcal{T}, \mathcal{D}_{10}, \mathcal{D}_6, C_5, \mathcal{D}_4, C_3, C_2$ and $\{e\}$, respectively.

In particular, this means that for any crystallographic representation of \mathcal{I} there are precisely $d_{\mathcal{G}}$ other such representations which share a subgroup isomorphic to \mathcal{G} . In other words, we can associate to the class $\mathcal{C}_{B_6}(\hat{\mathcal{I}})$ the ‘subgroup matrix’ S whose entries are defined by

$$S_{ij} = |\mathcal{H}_i \cap \mathcal{H}_j|, \quad i, j = 1, \dots, 192.$$

The matrix S is symmetric and $S_{ii} = 60$, for all i , since the order of \mathcal{I} is 60. It follows from Proposition 5.2 that each row of S contains $d_{\mathcal{G}}$ entries equal to $|\mathcal{G}|$. Moreover, a rearrangement of the columns of S shows that the 192 crystallographic representations of \mathcal{I} can be grouped into 12 sets of 16 such that any two of these representations in such a set of 16 share a \mathcal{D}_4 -subgroup. This implies that the corresponding subgraph of the \mathcal{D}_4 -graph is a complete graph, i.e. every two distinct vertices are connected by an edge. From a geometric point of view, these 16 representations correspond to ‘six-dimensional icosahedra’. This ensemble of 16 such icosahedra embedded into a six-dimensional hypercube can be viewed as a six-dimensional analogue of the three-dimensional ensemble of five tetrahedra inscribed into a dodecahedron, sharing pairwise a C_3 -subgroup.

We notice that, using Theorem 5.2, not all the graphs are connected. In particular, the \mathcal{D}_{10} - and the \mathcal{D}_6 -graphs are made up of six connected components, whereas the C_3 - and the C_2 -graphs consist of two connected components. With *GAP*, we implemented a breadth-first search algorithm (Foulds, 1992), which starts from a vertex i and then ‘scans’ for all the vertices connected to it, which allows us to find the connected components of a given \mathcal{G} -graph (see Appendix C). We find that each connected component of the \mathcal{D}_{10} - and \mathcal{D}_6 -graphs is made up of 32 vertices, while for the C_3 - and C_2 -graphs each component consists of 96 vertices. For all other subgroups, the corresponding \mathcal{G} -graph is connected and the connected component contains trivially 192 vertices.

We now consider in more detail the case when \mathcal{G} is a maximal subgroup of \mathcal{I} . Let $\mathcal{H} \in \mathcal{C}_{B_6}(\hat{\mathcal{I}})$ and let us consider its vertex star in the corresponding \mathcal{G} -graph, i.e.

$$V(\mathcal{H}) := \{\mathcal{K} \in \mathcal{C}_{B_6}(\hat{\mathcal{I}}) : \mathcal{K} \text{ is adjacent to } \mathcal{H}\}. \quad (15)$$

A comparison of Tables 5 and 6 shows that $d_{\mathcal{G}} = n_{\mathcal{G}}$ [i.e. the number of subgroups isomorphic to \mathcal{G} in \mathcal{I} , cf. equation (14)] and therefore, since the graph is regular, $|V(\mathcal{H})| = d_{\mathcal{G}} = n_{\mathcal{G}}$. This suggests that there is a one-to-one correspondence between elements of the vertex star of \mathcal{H} and subgroups of \mathcal{H} isomorphic to \mathcal{G} ; in other words, if we fix any subgroup P of \mathcal{H} isomorphic to \mathcal{G} , then P ‘connects’ \mathcal{H} with exactly another representation \mathcal{K} . We thus have the following:

Proposition 5.3. Let \mathcal{G} be a maximal subgroup of \mathcal{I} . Then for every $P \in \mathcal{C}_{B_6}(\mathcal{K}_G)$ there exist exactly two crystallographic representations of \mathcal{I} , $\mathcal{H}_1, \mathcal{H}_2 \in \mathcal{C}_{B_6}(\hat{\mathcal{I}})$, such that $P = \mathcal{H}_1 \cap \mathcal{H}_2$.

In order to prove it, we first need the following lemma:

Lemma 5.3. Let \mathcal{G} be a maximal subgroup of \mathcal{I} . Then the corresponding \mathcal{G} -graph is triangle-free, i.e. it has no circuits of length three.

Proof. Let $A_{\mathcal{G}}$ be the adjacency matrix of the \mathcal{G} -graph. By Theorem 5.1, its third power $A_{\mathcal{G}}^3$ determines the number of walks of length three, and in particular its diagonal entries, $(A_{\mathcal{G}}^3)_{ii}$, for $i = 1, \dots, 192$, correspond to the number of triangular circuits starting and ending in vertex i . A direct computation shows that $(A_{\mathcal{G}}^3)_{ii} = 0$, for all i , thus implying the non-existence of triangular circuits in the graph. \square

Proof of Proposition 5.3. If $P \in \mathcal{C}_{B_6}(\mathcal{K}_G)$, then, using Lemma 5.2, there exists $\mathcal{H}_1 \in \mathcal{C}_{B_6}(\hat{\mathcal{I}})$ such that P is a subgroup of \mathcal{H}_1 . Let us consider the vertex star $V(\mathcal{H}_1)$. We have $|V(\mathcal{H}_1)| = d_{\mathcal{G}}$; we call its elements $\mathcal{H}_2, \dots, \mathcal{H}_{d_{\mathcal{G}}+1}$. Let us suppose that P is not a subgroup of any \mathcal{H}_j , for $j = 2, \dots, d_{\mathcal{G}} + 1$. This implies that P does not connect \mathcal{H}_1 with any of these \mathcal{H}_j . However, since \mathcal{H}_1 has exactly $n_{\mathcal{G}}$ different subgroups isomorphic to \mathcal{G} , then at least two vertices in the vertex star, say \mathcal{H}_2 and \mathcal{H}_3 , are connected by the same subgroup isomorphic to \mathcal{G} , which we denote by Q . Therefore we have

$$Q = \mathcal{H}_1 \cap \mathcal{H}_2, Q = \mathcal{H}_1 \cap \mathcal{H}_3 \Rightarrow Q = \mathcal{H}_2 \cap \mathcal{H}_3.$$

This implies that $\mathcal{H}_1, \mathcal{H}_2$ and \mathcal{H}_3 form a triangular circuit in the graph, which is a contradiction due to Lemma 5.3, hence the result is proved. \square

It is noteworthy that the situation in B_6^+ is different. If we denote by X_1 and X_2 the two disjoint classes of crystallographic representations of \mathcal{I} in B_6^+ [cf. equation (13)], we can build, in the same way as described before, the \mathcal{G} -graphs for X_1 and X_2 , for $\mathcal{G} = \mathcal{T}, \mathcal{D}_{10}$ and \mathcal{D}_6 . The result is that the adjacency matrices of all these six graphs are the null matrix of dimension 96. This implies that these graphs have no edges, and so the representations in each class do not share any maximal subgroup of \mathcal{I} . As a consequence, we have the following:

Proposition 5.4. Let $\mathcal{H}, \mathcal{K} \in \mathcal{C}_{B_6}(\hat{\mathcal{I}})$ be two crystallographic representations of \mathcal{I} , and $P = \mathcal{H} \cap \mathcal{K}, P \in \mathcal{C}_{B_6}(\mathcal{K}_{\mathcal{G}})$, where \mathcal{G} is a maximal subgroup of \mathcal{I} . Then \mathcal{H} and \mathcal{K} are not conjugated in B_6^+ . In other words, the elements of B_6 which conjugate \mathcal{H} with \mathcal{K} are matrices with determinant equal to -1 .

We conclude by showing a computational method which combines the result of Propositions 4.1 and 5.2. We first recall the following:

Definition 5.1. Let H be a subgroup of a group G . The normaliser of H in G is given by

$$N_G(H) := \{g \in G : gHg^{-1} = H\}.$$

Corollary 5.1. Let \mathcal{H} and \mathcal{K} be two crystallographic representations of \mathcal{I} in B_6 and $P \in \mathcal{C}(\mathcal{K}_{\mathcal{G}})$ such that $P = \mathcal{H} \cap \mathcal{K}$. Let

$$A_{\mathcal{H},\mathcal{K}} = \{M \in B_6 : M\mathcal{H}M^{-1} = \mathcal{K}\}$$

be the set of all the elements of B_6 which conjugate \mathcal{H} with \mathcal{K} and let $N_{B_6}(P)$ be the normaliser of P in B_6 . We have

$$A_{\mathcal{H},\mathcal{K}} \cap N_{B_6}(H) \neq \emptyset.$$

In other words, it is possible to find a nontrivial element $M \in B_6$ in the normaliser of P in B_6 which conjugates \mathcal{H} with \mathcal{K} .

Proof. Let us suppose $A_{\mathcal{H},\mathcal{K}} \cap N_{B_6}(H) = \emptyset$. Then $MPM^{-1} \neq P$, for all $M \in A_{\mathcal{H},\mathcal{K}}$. This implies, since $M\mathcal{H}M^{-1} = \mathcal{K}$, that P is not a subgroup of \mathcal{K} , which is a contradiction. \square

We give now an explicit example. We consider the representation $\hat{\mathcal{I}}$ as in equation (12), and its subgroup $\mathcal{K}_{\mathcal{D}_{10}}$ (the explicit form is given in Appendix B). With GAP, we find the other representation $\mathcal{H}_0 \in \mathcal{C}(\hat{\mathcal{I}})$ such that $\mathcal{K}_{\mathcal{D}_{10}} = \hat{\mathcal{I}} \cap \mathcal{H}_0$. Its explicit form is given by

Table 6

Spectra of the \mathcal{G} -graphs for \mathcal{G} a nontrivial subgroup of \mathcal{I} and $\mathcal{G} = \{e\}$, the trivial subgroup consisting of only the identity element e .

The numbers highlighted are the indices of the graphs, and correspond to their degrees $d_{\mathcal{G}}$.

\mathcal{T} -graph		\mathcal{D}_{10} -graph		\mathcal{D}_6 -graph		\mathcal{C}_5 -graph	
Eig.	Mult.	Eig.	Mult.	Eig.	Mult.	Eig.	Mult.
5	1	6	6	10	6	0	192
3	45	2	90	2	90		
-3	45	-2	90	-2	90		
1	50	-6	6	-10	6		
-1	50						
-5	1						

\mathcal{D}_4 -graph		\mathcal{C}_3 -graph		\mathcal{C}_2 -graph		$\{e\}$ -graph	
Eig.	Mult.	Eig.	Mult.	Eig.	Mult.	Eig.	Mult.
30	1	20	2	60	2	60	1
18	5	4	90	4	90	12	5
12	5	-4	100	-4	90	4	90
6	15			-12	10	-4	90
2	45					-12	5
0	31					-60	1
-2	30						
-4	45						
-8	15						

$$\mathcal{H}_0 = \left\langle \begin{pmatrix} 0 & 0 & 0 & 0 & -1 & 0 \\ 0 & 0 & 0 & 1 & 0 & 0 \\ 0 & 0 & -1 & 0 & 0 & 0 \\ 0 & 1 & 0 & 0 & 0 & 0 \\ -1 & 0 & 0 & 0 & 0 & 0 \\ 0 & 0 & 0 & 0 & 0 & -1 \end{pmatrix}, \begin{pmatrix} 0 & 0 & 0 & 0 & -1 & 0 \\ 0 & 0 & -1 & 0 & 0 & 0 \\ 0 & 0 & 0 & 0 & 0 & 1 \\ 1 & 0 & 0 & 0 & 0 & 0 \\ 0 & 0 & 0 & -1 & 0 & 0 \\ 0 & -1 & 0 & 0 & 0 & 0 \end{pmatrix} \right\rangle.$$

A direct computation shows that the matrix

$$M = \begin{pmatrix} 1 & 0 & 0 & 0 & 0 & 0 \\ 0 & -1 & 0 & 0 & 0 & 0 \\ 0 & 0 & 1 & 0 & 0 & 0 \\ 0 & 0 & 0 & 1 & 0 & 0 \\ 0 & 0 & 0 & 0 & 1 & 0 \\ 0 & 0 & 0 & 0 & 0 & 1 \end{pmatrix}$$

belongs to $N_{B_6}(\mathcal{K}_{\mathcal{D}_{10}})$ and conjugate $\hat{\mathcal{I}}$ with \mathcal{H}_0 . Note that $\det M = -1$.

6. Conclusions

In this work we explored the subgroup structure of the hyperoctahedral group in six dimensions. In particular we found the class of the crystallographic representations of the icosahedral group, whose size is 192. Any such representation, together with its corresponding projection operator π^{\parallel} , can be chosen to construct icosahedral quasicrystals *via* the cut-and-project method. We then studied in detail the subgroup structure of this class. For this, we proposed a method based on spectral graph theory and introduced the concept of \mathcal{G} -graph, for a subgroup \mathcal{G} of the icosahedral group. This allowed us to study the intersection and the subgroups shared by different representations. We have shown that, if we fix any repre-

sensation \mathcal{H} in the class and a maximal subgroup P of \mathcal{H} , then there exists exactly one other representation \mathcal{K} in the class such that $P = \mathcal{H} \cap \mathcal{K}$. As explained in the *Introduction*, this can be used to describe transitions which keep intermediate symmetry encoded by P . In particular, this result implies in this context that a transition from a structure arising from \mathcal{H} via projection will result in a structure obtainable for \mathcal{K} via projection if the transition has intermediate symmetry described by P . Therefore, this setting is the starting point to analyse structural transitions between icosahedral quasicrystals, following the methods proposed in Kramer (1987), Katz (1989) and Indelicato *et al.* (2012), which we are planning to address in a forthcoming publication.

These mathematical tools also have many applications in other areas. A prominent example is virology. Viruses package their genomic material into protein containers with regular structures that can be modelled via lattices and group theory. Structural transitions of these containers, which involve rearrangements of the protein lattices, are important in rendering certain classes of viruses infective. As shown in Indelicato *et al.* (2011), such structural transitions can be modelled using projections of six-dimensional icosahedral lattices and their symmetry properties. The results derived here therefore have a direct application to this scenario, and the information on the subgroup structure of the class of crystallographic representations of the icosahedral group and their intersections provides information on the symmetries of the capsid during the transition.

APPENDIX A

In order to render this paper self-contained, we provide the character tables of the subgroups of the icosahedral group, following Artin (1991), Fulton & Harris (1991) and Jones (1990).

Tetrahedral group \mathcal{T} [$\omega = \exp(2\pi i/3)$]:

Irrep	$C(e)$	$4C_3$	$4C_3^2$	$3C_2$
A	1	1	1	1
E	1	ω	ω^2	1
	1	ω^2	ω	1
T	3	0	0	-1

Dihedral group \mathcal{D}_{10} :

Irrep	E	$2C_5$	$2C_5^2$	$5C_2$
A_1	1	1	1	1
A_2	1	1	1	-1
E_1	2	$\tau-1$	$-\tau$	0
E_2	2	$-\tau$	$\tau-1$	0

Dihedral group \mathcal{D}_6 (isomorphic to the symmetric group S_3):

Irrep	E	$3C_2$	$2C_3$
A_1	1	1	1
A_2	1	-1	1
E	2	0	-1

Cyclic group C_5 [$\epsilon = \exp(2\pi i/5)$]:

Irrep	e	C_5	C_5^2	C_5^3	C_5^4
A	1	1	1	1	1
E_1	1	ϵ	ϵ^2	ϵ^{2*}	ϵ^*
	1	ϵ^*	ϵ^{2*}	ϵ^2	ϵ
E_2	1	ϵ^2	ϵ^*	ϵ	ϵ^{2*}
	1	ϵ^{2*}	ϵ	ϵ^*	ϵ^2

Dihedral group D_4 (the Klein Four Group):

Irrep	E	C_{2x}	C_{2y}	C_{2z}
A	1	1	1	1
B_1	1	1	-1	-1
B_2	1	-1	1	-1
B_3	1	-1	-1	1

Cyclic group C_3 [$\omega = \exp(2\pi i/3)$]:

Irrep	E	C_3	C_3^2
A	1	1	1
E	1	ω	ω^2
	1	ω^2	ω

Cyclic group C_2 :

Irrep	E	C_2
A	1	1
B	1	-1

APPENDIX B

Here we show the explicit forms of \mathcal{K}_g , the representations in B_6 of the subgroups of \mathcal{I} , together with their decompositions in $GL(6, \mathbb{R})$.

$$\mathcal{K}_{\mathcal{T}} = \left\langle \begin{pmatrix} 0 & 0 & 0 & 0 & 0 & 1 \\ 0 & 0 & 0 & 0 & 1 & 0 \\ 0 & 0 & -1 & 0 & 0 & 0 \\ 0 & 0 & 0 & -1 & 0 & 0 \\ 0 & 1 & 0 & 0 & 0 & 0 \\ 1 & 0 & 0 & 0 & 0 & 0 \end{pmatrix}, \begin{pmatrix} 0 & 1 & 0 & 0 & 0 & 0 \\ 0 & 0 & 0 & -1 & 0 & 0 \\ 0 & 0 & 0 & 0 & 0 & -1 \\ -1 & 0 & 0 & 0 & 0 & 0 \\ 0 & 0 & 1 & 0 & 0 & 0 \\ 0 & 0 & 0 & 0 & -1 & 0 \end{pmatrix} \right\rangle,$$

$$\mathcal{K}_{\mathcal{D}_{10}} = \left\langle \begin{pmatrix} 0 & 0 & 0 & 0 & 0 & -1 \\ 0 & -1 & 0 & 0 & 0 & 0 \\ 0 & 0 & 0 & 1 & 0 & 0 \\ 0 & 0 & 1 & 0 & 0 & 0 \\ 0 & 0 & 0 & 0 & -1 & 0 \\ -1 & 0 & 0 & 0 & 0 & 0 \end{pmatrix}, \begin{pmatrix} 0 & 0 & 0 & 0 & 0 & 1 \\ 0 & 1 & 0 & 0 & 0 & 0 \\ 0 & 0 & 0 & 0 & -1 & 0 \\ -1 & 0 & 0 & 0 & 0 & 0 \\ 0 & 0 & 0 & 1 & 0 & 0 \\ 0 & 0 & 1 & 0 & 0 & 0 \end{pmatrix} \right\rangle,$$

$$\mathcal{K}_{\mathcal{D}_6} = \left\langle \begin{pmatrix} 0 & 0 & 0 & 0 & 0 & -1 \\ 0 & -1 & 0 & 0 & 0 & 0 \\ 0 & 0 & 0 & 1 & 0 & 0 \\ 0 & 0 & 1 & 0 & 0 & 0 \\ 0 & 0 & 0 & 0 & -1 & 0 \\ -1 & 0 & 0 & 0 & 0 & 0 \end{pmatrix}, \begin{pmatrix} 0 & 0 & 0 & 0 & 0 & 1 \\ 0 & 0 & 0 & 1 & 0 & 0 \\ 0 & -1 & 0 & 0 & 0 & 0 \\ 0 & 0 & -1 & 0 & 0 & 0 \\ 1 & 0 & 0 & 0 & 0 & 0 \\ 0 & 0 & 0 & 0 & 1 & 0 \end{pmatrix} \right\rangle,$$

$$\mathcal{K}_{C_5} = \left\langle \begin{pmatrix} 0 & 0 & 0 & 0 & 0 & 1 \\ 0 & 1 & 0 & 0 & 0 & 0 \\ 0 & 0 & 0 & 0 & -1 & 0 \\ -1 & 0 & 0 & 0 & 0 & 0 \\ 0 & 0 & 0 & 1 & 0 & 0 \\ 0 & 0 & 1 & 0 & 0 & 0 \end{pmatrix} \right\rangle,$$

$$\mathcal{K}_{D_4} = \left\langle \begin{pmatrix} 0 & 0 & 0 & 0 & 0 & -1 \\ 0 & -1 & 0 & 0 & 0 & 0 \\ 0 & 0 & 0 & 1 & 0 & 0 \\ 0 & 0 & 1 & 0 & 0 & 0 \\ 0 & 0 & 0 & 0 & -1 & 0 \\ -1 & 0 & 0 & 0 & 0 & 0 \end{pmatrix}, \begin{pmatrix} 0 & 0 & 0 & 0 & 0 & 1 \\ 0 & 0 & 0 & 0 & 1 & 0 \\ 0 & 0 & -1 & 0 & 0 & 0 \\ 0 & 0 & 0 & -1 & 0 & 0 \\ 0 & 1 & 0 & 0 & 0 & 0 \\ 1 & 0 & 0 & 0 & 0 & 0 \end{pmatrix} \right\rangle,$$

$$\mathcal{K}_{C_3} = \left\langle \begin{pmatrix} 0 & 0 & 0 & 0 & 0 & 1 \\ 0 & 0 & 0 & 1 & 0 & 0 \\ 0 & -1 & 0 & 0 & 0 & 0 \\ 0 & 0 & -1 & 0 & 0 & 0 \\ 1 & 0 & 0 & 0 & 0 & 0 \\ 0 & 0 & 0 & 0 & 1 & 0 \end{pmatrix} \right\rangle,$$

$$\mathcal{K}_{C_2} = \left\langle \begin{pmatrix} 0 & 0 & 0 & 0 & 0 & 1 \\ 0 & 0 & 0 & 0 & 1 & 0 \\ 0 & 0 & -1 & 0 & 0 & 0 \\ 0 & 0 & 0 & -1 & 0 & 0 \\ 0 & 1 & 0 & 0 & 0 & 0 \\ 1 & 0 & 0 & 0 & 0 & 0 \end{pmatrix} \right\rangle.$$

$$\mathcal{K}_T \simeq 2T, \mathcal{K}_{D_{10}} \simeq 2A_2 \oplus E_1 \oplus E_2, \mathcal{K}_{D_6} \simeq 2A_2 \oplus 2E, \mathcal{K}_{C_5} \simeq 2A \oplus E_1 \oplus E_2,$$

$$\mathcal{K}_{D_4} \simeq 2B_1 \oplus 2B_2 \oplus 2B_3, \mathcal{K}_{C_3} \simeq 2A \oplus 2E, \mathcal{K}_{C_2} \simeq 2A \oplus 4B.$$

APPENDIX C

In this Appendix we show our algorithms, which have been implemented in *GAP* and used in various sections of the paper. We list them with a number from 1 to 5.

Algorithm 1 (Fig. 2): Classification of the crystallographic representations of \mathcal{I} (see §4). The algorithm carries out steps 1–4 used to prove Proposition 4.1. In the *GAP* computation, the class $\mathcal{C}_{B_6}(\hat{\mathcal{I}})$ is indicated as CB6s60. Its size is 192.

Algorithm 2 (Fig. 3): Computation of the vertex star of a given vertex i in the \mathcal{G} -graphs. In the following, H stands for the class $\mathcal{C}_{B_6}(\hat{\mathcal{I}})$ of the crystallographic representations of \mathcal{I} , $i \in \{1, \dots, 192\}$ denotes a vertex in the \mathcal{G} -graph corresponding to the representation $H[i]$ and n stands for the size of \mathcal{G} : we can use the size instead of the explicit form of the subgroup since, in the case of the icosahedral group, all the non isomorphic subgroups have different sizes.

Algorithm 3 (Fig. 4): Computation of the adjacency matrix of the \mathcal{G} -graph.

Algorithm 4 (Fig. 5): This algorithm carries out a breadth-first search strategy for the computation of the connected component of a given vertex i of the \mathcal{G} -graph.

Algorithm 5 (Fig. 6): Computation of all connected components of a \mathcal{G} -graph.

```
gap > B6:= Group([(1,2)(7,8),(1,2,3,4,5,6)(7,8,9,10,11,12),(6,12)]);
gap > C:= ConjugacyClassesSubgroups(B6);
gap > C60:= Filtered(C,x->Size(Representative(x))=60);
gap > Size(C60);
3
gap > s60:= List(C60,Representative);
gap > I:= AlternatingGroup(5);
gap > IsomorphismGroups(I,s60[1]);
[(2,4)(3,5),(1,2,3)]->[(1,3)(2,4)(7,9)(8,10),(3,10,11)(4,5,9)]
gap > IsomorphismGroups(I,s60[2]);
[(2,4)(3,5),(1,2,3)]->[(1,2)(3,10)(4,9)(5,11)(6,12)(7,8),
(1,2,4)(3,12,5)(6,11,9)(7,8,10)]
gap > IsomorphismGroups(I,s60[3]);
[(2,4)(3,5),(1,2,3)]->[(2,6)(4,11)(5,10)(8,12),
(1,3,5)(2,4,6)(7,9,11)(8,10,12)]
gap > CB6s60:= ConjugacyClassSubgroups(B6,s60[2]);
gap > Size(CB6s60);
192
```

Figure 2
Algorithm 1.

```
gap > VertexStar :=function(H,i,n)
> local j,R,S;
> R:=[];
> for j in [1..Size(H)] do
> S:=Intersection(H[i],H[j]);
> if Size(S) = n then
> R:=Concatenation(R,[j]);
> fi;
> od;
> return R;
> end;
```

Figure 3
Algorithm 2.

```
gap > AdjacencyMatrix:=function(H,n)
> local i,j,C,A;
> A:=NullMat(Size(H),Size(H));
> for i in [1..Size(H)] do
> C:=VertexStar(H,i,n);
> for j in [1..Size(C)] do
> A[i][C[j]]:=1;
> od;
> od;
> return A;
> end;
```

Figure 4
Algorithm 3.

```

gap> ConnectedComponent:=function(H,i,n)
> local R,S,T,j,k,C;
> R:=[];
> S:=[];
> while Size(S) <= Size(H) do
> T:=[];
> for j in [1..Size(R)] do
> C:=VertexStar(H,R[j],n);
> for k in [1..Size(C)] do
> if (C[k] in S) = false then
> Add(S,C[k]);
> T:=Concatenation(T,[C[k]]);
> fi;
> od;
> od;
> if T = [] then return S;
> else
> R:=T;
> fi;
> od;
> return S;
> end;

```

Figure 5
Algorithm 4.

We would like to thank Silvia Steila, Pierre-Philippe Dechant, Paolo Cermelli and Giuliana Indelicato for useful discussions, and Paolo Barbero and Alessandro Marchino for technical help. ECD thanks the Leverhulme Trust for an Early Career Fellowship (ECF-2013-019) and the EPSRC for funding (EP/K02828671).

References

Artin, M. (1991). *Algebra*. New York: Prentice Hall.
 Baake, M. (1984). *J. Math. Phys.* **25**, 3171–3182.
 Baake, M. & Grimm, U. (2013). *Aperiodic Order*, Vol. 1. Cambridge University Press.
 Cvetkovic, D., Doob, M. & Sachs, H. (1995). *Spectra of Graphs*. Heidelberg, Leipzig: Johann Ambrosius Barth.
 Foulds, L. (1992). *Graph Theory Applications*. New York: Springer-Verlag.
 Fulton, W. & Harris, J. (1991). *Representation Theory: A First Course*. Springer-Verlag.
 Horn, R. & Johnson, C. (1985). *Matrix Analysis*. Cambridge University Press.

```

gap> ConnectedComponents:=function(H,n)
> local j,S,C;
> C:=[];
> S:=Flat(C);
> if Size(S) = Size(H) then return S;
> fi;
> for j in [1..Size(H)] do
> if (j in S) = false then
> C:=Concatenation(C,[ConnectedComponent(H,j,n)]);
> S:=Flat(C);
> if Size(S) = Size(H) then return C;
> fi;
> fi;
> od;
> end;

```

Figure 6
Algorithm 5.

Hoyle, R. (2004). *Physica D*, **191**, 261–281.
 Humphreys, J. (1990). *Reflection Groups and Coxeter Groups*. Cambridge University Press.
 Humphreys, J. (1996). *A Course in Group Theory*. Oxford University Press.
 Indelicato, G., Cermelli, P., Salthouse, D., Racca, S., Zanzotto, G. & Twarock, R. (2011). *J. Math. Biol.* **64**, 745–773.
 Indelicato, G., Keef, T., Cermelli, P., Salthouse, D., Twarock, R. & Zanzotto, G. (2012). *Proc. R. Soc. A*, **468**, 1452–1471.
 Janusz, G. & Rotman, J. (1982). *Am. Math. Mon.* **89**, 407–410.
 Jones, H. (1990). *Groups, Representations and Physics*. Institute of Physics Publishing.
 Katz, A. (1989). In *Introduction to the Mathematics of Quasicrystals*, edited by M. Jarić. New York: Academic Press.
 Kramer, P. (1987). *Acta Cryst.* **A43**, 486–489.
 Kramer, P. & Haase, R. (1989). In *Introduction to the Mathematics of Quasicrystals*, edited by M. Jarić. New York: Academic Press.
 Kramer, P. & Zeidler, D. (1989). *Acta Cryst.* **A45**, 524–533.
 Levitov, L. & Rhyner, J. (1988). *J. Phys. France*, **49**, 1835–1849.
 Moody, R. (2000). In *From Quasicrystals to More Complex Systems*, edited by F. Axel, F. Dénoyer & J. P. Gazeau. Springer-Verlag.
 Pitteri, M. & Zanzotto, G. (2002). *Continuum Models for Phase Transitions and Twinning in Crystals*. London: CRC/Chapman and Hall.
 Senechal, M. (1995). *Quasicrystals and Geometry*. Cambridge University Press.
 Soicher, L. (2006). *Oberwolfach Rep.* **3**, 1809–1811. Report 30/2006.
 Steurer, W. (2004). *Z. Kristallogr.* **219**, 391–446.
 The GAP Group (2013). *GAP – Groups, Algorithms, and Programming*, Version 4.7.2. <http://www.gap-system.org>.
 Zappa, E., Indelicato, G., Albano, A. & Cermelli, P. (2013). *Int. J. Non-Linear Mech.* **56**, 71–78.